JCTC Journal of Chemical Theory and Computation

Article

pubs.acs.org/JCTC

Automated Search for Minimum Energy Conical Intersection Geometries between the Lowest Two Singlet States S_0/S_1-MECIs by the Spin-Flip TDDFT Method

Yu Harabuchi,[†] Satoshi Maeda,*[,†] Tetsuya Taketsugu,[†] Noriyuki Minezawa,[‡] and Keiji Morokuma*[,‡,§]

[†]Department of Chemistry, Faculty of Science, Hokkaido University, Sapporo 060-0810, Japan

[‡]Fukui Institute for Fundamental Chemistry, Kyoto University, 34-4 Takano Nishihiraki-cho, Sakyo, Kyoto 606-8103, Japan

[§]Cherry L. Emerson Center for Scientific Computation and Department of Chemistry, Emory University, Atlanta, Georgia 30322, United States

Supporting Information

ABSTRACT: Automated search for minimum energy conical intersection geometries between the lowest two singlet states (S_0/S_1-MECIs) was performed by combining the anharmonic downward distortion following (ADDF) method, the seam model function (SMF) approach, and the spin-flip (SF) TDDFT method. SMF/ADDF has been employed previously in automated searches for MECIs on potential energy surfaces (PESs) with expensive multireference methods. In this work, we adopt the SF-TDDFT method that enables efficient optimization of S_0/S_1-MECIs in the framework of TDDFT. To evaluate the performance of the present approach, it was applied to ethylene and 1,3-butadiene. The present method automatically gave unknown S_0/S_1-MECIs as well as all previously reported ones. Therefore, the present hybrid method of SMF/ADDF and SF-TDDFT is shown to be a promising approach to locate S_0/S_1-MECIs of large systems automatically with modest computational costs.

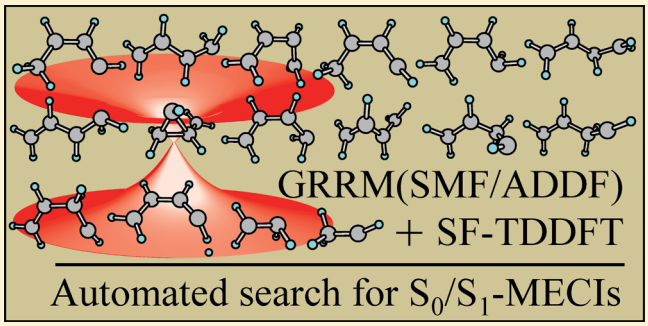

I. INTRODUCTION

The theoretical calculation has become a powerful tool in studying the mechanism of photochemical reactions. In many photochemical reactions, nonadiabatic transitions through the conical intersections (CIs) play a key role.[1−7] The CI is an (f − 2)-dimensional intersection hyperspace between two or more potential energy surfaces (PESs) for states having the same spin and space symmetry, where f is the number of degrees of freedom. In the Franck−Condon (FC) principle, it is assumed that dynamics starts from the FC point. If a CI region is accessible from the FC point by a given total energy, the system can decay efficiently to the lower electronic states by nonadiabatic transitions. If there is no accessible CI, the nonradiative decay will be slow and the system exhibits a high fluorescence quantum yield. One can predict whether there is an accessible CI or not, by locating all low-lying minimum-energy CI (MECI) geometries. One notes that there is also (f − 1)-dimensional seam of crossing (SX) hypersurface between states with different spin states. Accessible low-lying minimum-energy SX (MESX) geometries account for efficient intersystem crossing processes.

Various methods have been developed for geometry optimization of the MECIs.[8−16] These can be classified into three types: constrained optimization methods,[8,9,11] the direct gradient (DG) method,[10,15,16] and penalty function (PF) methods.[12,14] A systematic comparison revealed that the former two converge faster than the PF method.[13] There is a significant advantage in PF methods that derivative coupling vector (DCV) calculations are not required in MECI optimizations. Calculations of DCV can be avoided also by using the branching plane (BP) updating method in combination with constrained optimization methods and the DG method.[16] These methods have been successfully applied to many photochemical reactions. However, in general, these geometry optimization methods require a good initial guess. Guessing the MECI structures generally is not an easy task, because their geometrical features are often highly deviated from those of stable molecular structures in the electronic ground state. Thus, a method that can search for all MECIs automatically has been required.

There has been a similar problem in the reaction path search, in which finding all important transition state (TS) structures is often very difficult. Recently, Maeda et al. have developed two methods for finding reaction pathways as well as associated local minima and TSs automatically without needing any guess:[17] the anharmonic downward distortion following (ADDF) method[18−20] and the artificial force induced reaction

Received: June 17, 2013
Published: July 22, 2013

   dx.doi.org/10.1021/ct400512u | J. Chem. Theory Comput. 2013, 9, 4116−4123

(AFIR) method.[21−23] ADDF can find isomerization and dissociation channels starting from local minima. AFIR can efficiently explore addition reaction paths among multiple reactants. Very recently, a simple recipe has been proposed for exploring multiple PESs automatically, and the recipe in combination with ADDF and AFIR enabled automated search for MECIs and TSs in the electronic excited states.[24−26] The recipe has been applied to various photochemical reactions of small molecules on the basis of multiconfigurational or multireference calculations, such as CASSCF and CASPT2. However, energetics by CASSCF are often poor, because of the omission of a majority of the dynamic electron correlation. Although inclusion of dynamic correlations is often necessary for the better energetics as well as geometries at MECIs,[27,28] even the widely used CASPT2 method can be highly demanding in large systems especially when many MECIs are searched by ADDF and AFIR. Thus, the TDDFT method, which is an efficient alternative to include dynamic correlations, is considered in this study.

TDDFT has been employed extensively in describing the PESs of excited states.[29−31] TDDFT calculations can take account of dynamic correlations with much lower costs, compared to CASPT2. However, TDDFT has several disadvantages.[32] First, the linear-response TDDFT within the adiabatic approximation cannot describe doubly excited configurations. Second, the PES derived by TDDFT calculations is not continuous around CI regions between the reference (ground singlet S_0) state and the first excited singlet S_1 state, because the reference state becomes higher in energy than the response state around the S_0/S_1−CI region. The latter makes optimization of the MECIs between S_0 and S_1 very difficult. Recently, the spin-flip TDDFT (SF-TDDFT) method has been developed to overcome these problems.[33−40] In SF-TDDFT, instead of S_0, the lowest triplet T_1 state with two unpaired alpha electrons is used as the reference. This allows one to describe the HOMO−LUMO doubly excited state. Moreover, the S_0 and S_1 states can be described correctly around the S_0/S_1−CI region, because the SF-TDDFT treats both states on an equal footing as the response states. Consequently, PESs of the singlet states become continuous near S_0/S_1−CI regions. Very recently, the analytical gradient of the SF-TDDFT was implemented, and it has been successfully employed in optimizations of S_0/S_1-MECI geometries.[35] It was also demonstrated in oxirane that the correct branching plane can be reproduced by SF-TDDFT.[36]

In this paper, we focus on the automated and systematic global search for S_0/S_1-MECIs with the SF-TDDFT method, in combination with the ADDF method. In the actual implementation, however, we need to pay attention to the following points. The response states are not the spin eigenstates because spin-flip excitations do not always form spin-adapted configurations. In addition, the root flipping occurs frequently during the MECI optimization. These problems sometimes made it difficult to choose S_0 and S_1 states automatically from low-lying states with significant spin contaminations, and this was consequently an obstacle in the automated MECI searches. To overcome this problem, we introduce a simple but robust approach. To evaluate the performance of the present approach, it was applied to MECI searches of two unsaturated hydrocarbons: ethylene and butadiene. Since these two systems have been studied thoroughly,[14,15,32,33,35,41−65] on the basis of multireference calculations, they can be reasonable test systems.

II. THEORY

A. Anharmonic Downward Distortion Following (ADDF). ADDF method has been developed to follow reaction pathways starting from local minima on a PES toward TSs and dissociation channels (DCs).[18−20] Since typical reaction paths always change their curvatures from concave to convex upon going to a TS or a DC, slopes should always decline from the respective harmonic curve, because of energy-lowering interactions, leading to a TS or a DC. Therefore, by following ADD maximal directions, reaction pathways can be followed from a local minimum ratio of TSs and DCs. Once a TS is found, the intrinsic reaction coordinate[66] is used to determine the next local minimum to which the TS connects. In the standard algorithm, all possible ADD-maximal pathways are followed, starting from all obtained local minima, and a network of reaction pathways is constructed. This has been done for ground-state molecules consisting of ∼10 atoms,[17] but the process would become very expensive for larger molecules. In many applications, high-energy local minima and TSs are not required. In such cases, one can use the large ADD following (*l*-ADDF*n*) algorithm, in which only largest *n* ADD directions are considered.[67] In the present study, *l*-ADDF3 is adopted, in order to find the three lowest pathways within the seam of intersection hyperspaces. Further details on the ADDF method are described in a recent review.[17]

B. Seam Model Function Approach. In order to achieve the automated search for MECIs, the ADDF method is applied to the following model function.[24,25]

$$F^{\mathrm{SMF}}(\mathbf{Q}) = \frac{1}{2}(E^{\mathrm{State}\,1}(\mathbf{Q}) + E^{\mathrm{State}\,2}(\mathbf{Q})) + \frac{(E^{\mathrm{State}\,1}(\mathbf{Q}) - E^{\mathrm{State}\,2}(\mathbf{Q}))^2}{\beta} \quad (1)$$

Equation 1 consists of two terms: the mean potential energy of two electronic states and a penalty function that adds a penalty depending on their energy gap. $\mathbf{Q}$ is the atomic coordinates $\{Q_i\}$, $E^{\mathrm{State}\,1}(\mathbf{Q})$ and $E^{\mathrm{State}\,2}(\mathbf{Q})$ are PESs of two target states, and β is a constant parameter. Minimization of F^{SMF} gives a geometry in which both the mean energy of the two states (the first term) and the energy gap between the two states (the second term) are small. Hence, minima of F^{SMF} would provide good guesses of MECIs. Although smaller β gives better (more accurate) candidates, minimizations of F^{SMF} with smaller β require more optimization steps. In this study, β is set to a standard value[24] of 30 kJ/mol throughout. Local minima on the above model function, i.e., *approximate* MECIs, can systematically be searched by ADDF. Then, these *approximate* structures are optimized to *true* MECIs using a standard MECI optimization method, and, in this study, the DG method was employed, in combination with the BP-updating method. We call this two-step approach for finding MECIs automatically *the seam model function (SMF) approach*. We note that different electronic structure methods can be used in these two steps, e.g., initial automated search for *approximate* MECIs by SF-TDDFT and reoptimization of *true* MECIs by CASPT2. It should be emphasized that DCVs are not required at all in the present search procedure, since we have designed our search algorithms so that DCV calculations can be totally avoided.

C. Spin-Flip TDDFT. The SF-TDDFT method can treat all excited states that are expressed by linear combinations of Slater determinants obtained by one-electron transitions accompanied with the α-to-β spin flip from the reference T_1

state. From the reference T_1 state shown in Figure 1a, nine different types of Slater determinants (shown in Figures 1b–f

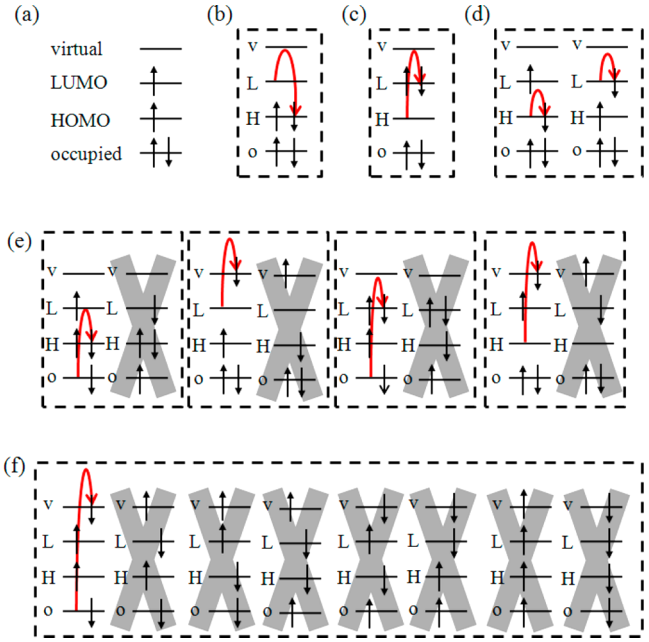

Figure 1. All possible Slater determinants obtained by one-electron spin-flip excitations from the reference triplet state (shown without gray crosses) and missing counterparts of configuration state functions (shown with gray crosses): (a) the reference state, (b) the singlet ground state, (c) the [HOMO → LUMO] doubly excited state, (d) the [HOMO → LUMO] singly excited states, (e and f) excited states involving o and v orbitals.

without gray crosses) can be generated by one-electron spin-flip excitations (only four molecular orbitals, HOMO (H), LUMO (L), virtual orbital (v), and occupied orbital (o), are shown in Figure 1 for the sake of clarity). In Figures 1e and 1f, there are some missing counterparts of configuration state functions (CSFs), shown by determinants with gray crosses. Therefore, spin eigenstates of excited states of the types depicted in panels (e) and (f) from Figure 1 cannot be described in the SF-TDDFT framework.

As shown in Figures 1b and 1c, respectively, the singlet ground state and the [HOMO → LUMO] doubly excited state can be described. The CSFs for the open-shell singlet and triplet states related to the [HOMO → LUMO] one-electron excitation, shown in Figure 1d, can also be described by the linear combination of two configurations: $|\mathrm{HOMO}_\alpha\cdot\mathrm{LUMO}_\beta\rangle \pm |\mathrm{HOMO}_\beta\cdot\mathrm{LUMO}_\alpha\rangle$. On the other hand, CSFs of the types shown in Figures 1e and f types are incomplete in SF-TDDFT, because of the missing Slater determinants, as indicated by gray crosses. As a result, SF-TDDFT gives solutions with unphysical $\langle \mathbf{S}^2\rangle$ spin expectation values. States of the type depicted in Figure 1e are singlet/triplet mixed states and typically give $\langle \mathbf{S}^2\rangle \approx 1.0$. Those of the type described in Figure 1f type show $\langle \mathbf{S}^2\rangle > 2.0$, because of contamination by the quintet states; in our experience, this type does not appear frequently in calculations of low-lying states. These problematic configurations correspond to the open-shell singlet states involving excitations to v orbitals and/or from o orbitals. In other words, SF-TDDFT can describe only the [HOMO → LUMO] one-electron excitation and doubly excited state properly.

This problem will be serious, especially in automated exploration of wide areas of the PES, since it may be very difficult to choose correct target states automatically. In calculations of low-lying states, three types of spin states, i.e., singlet states with $\langle \mathbf{S}^2\rangle \approx 0.0$, triplet states with $\langle \mathbf{S}^2\rangle \approx 2.0$, and singlet/triplet mixed states $\langle \mathbf{S}^2\rangle \approx 1.0$, appear, as discussed above. Previously, it was reported that deviations from the ideal $\langle \mathbf{S}^2\rangle$ values are usually <0.2 at optimized local minimum and MECI structures.[39] This is encouraging, since one can choose correct target states automatically on the basis of $\langle \mathbf{S}^2\rangle$ values. At first, we considered an approach in which gradients for S_0 and S_1 were obtained in the three steps: (1) perform a single-point calculation, (2) choose the lowest two states with $\langle \mathbf{S}^2\rangle \leq 0.5$, and (3) compute gradients for the chosen states. However, such an approach often failed when the value of $\langle \mathbf{S}^2\rangle$ goes beyond 0.5 from <0.5 and/or when it changed largely with small geometrical displacements during automated exploration. The latter was especially serious since it caused unwanted oscillations of search steps due to exchanges of target states. These problematic cases are seen when HOMO and HOMO−1 (or LUMO and LUMO+1) are nearly degenerate, since $\langle \mathbf{S}^2\rangle$ values of SF-TDDFT become close to the ideal values 0.0 and 2.0 only in states described by HOMO → LUMO excitations. During automated searches, we sometimes encountered very difficult cases in which all the three or four lowest states have $\langle \mathbf{S}^2\rangle \approx 1.0$. Although the use of Yamaguchi's approximate spin projection formula[68,69] may be a solution to this problem, as has been proposed recently,[70] it cannot be readily applied to such very difficult cases. In order to achieve the automated global search, one must choose the most robust strategy in which the search will never be interrupted by the spin-state ambiguity problem.

Hence, an alternative strategy was introduced in this study. In the strategy, it is abandoned to distinguish spin states during automated searches. Instead, all the lowest *m*-states are considered, and minima of F^{SMF} in eq 1 for all the neighboring pairs of PESs are searched using the SMF/ADDF approach. The lowest four PESs (PES-I, PES-II, PES-III, and PES-IV) were considered in this study not to overlook low-lying S_0/S_1-MECIs on the assumption that the S_0 and S_1 states can be assigned to one of the first four roots. In other words, SMF/ADDF was applied to PES-I/PES-II, PES-II/PES-III, and PES-III/PES-IV. By an application of this strategy, MESX structures including MECIs for these four surfaces can be obtained automatically. Finally, these MESXs can be classified into S_0/S_1-MECIs, S_0/T_1-MESXs, S_1/T_1-MESXs, etc. afterward, based on the $\langle \mathbf{S}^2\rangle$ values at optimized structures. As demonstrated below, we have accomplished the automated global search for MECIs using this strategy.

III. COMPUTATIONAL DETAILS

The present approach was applied to ethylene and 1,3-butadiene. In the initial SMF/ADDF search (the first step of SMF), the BHHLYP (50% Hartree−Fock plus 50% Becke exchange[71] with Lee−Yang−Parr correlation)[72] functional and the 6-31G basis set were employed in SF-TDDFT calculations (indicated as SF-BHHLYP/6-31G). In all the SF-TDDFT calculations, reference triplet states were calculated based on the spin-unrestricted framework, and the collinear approximation[33] was used. The SMF/ADDF searches were started from the ground-state ethylene and the ground-state *cis*- and *trans*-1,3-butadiene structures. To reduce computational costs by restricting the search area to be low-energy regions, the *l*-

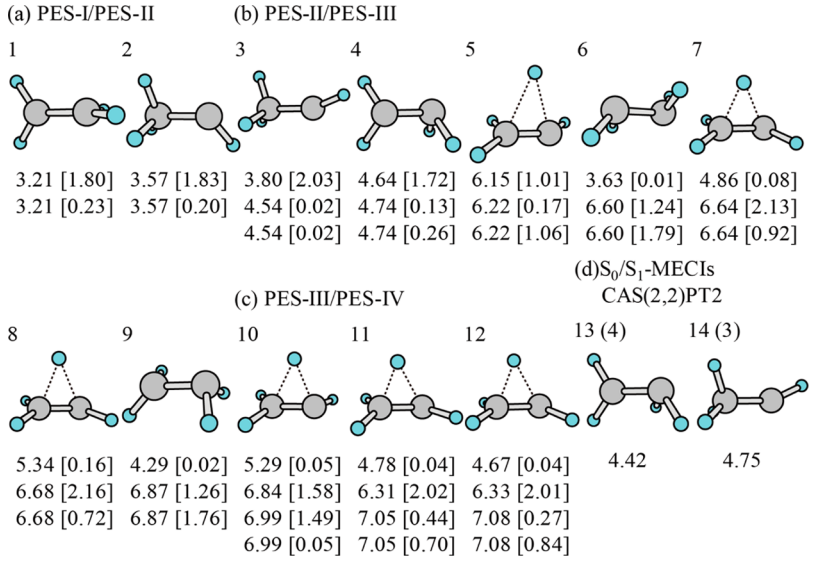

Figure 2. Structures and energies of lowest two to four states at the optimized MESXs (including MECIs) at the SF-BHHLYP/cc-pVDZ level and at the optimized S_0/S_1-MECIs at the MS3-CAS(2e,2o)PT2/cc-pVDZ level for C_2H_4: (a) PES-I/PES-II MESXs, (b) PES-II/PES-III MESXs, (c) PES-III/PES-IV MESXs at the SF-BHHLYP/cc-pVDZ level, and (d) S_0/S_1-MECIs at the CASPT2 level. Energies (in eV) are relative to the ground-state ethylene, and $\langle S^2 \rangle$ values for corresponding states are shown in square brackets. In structure labels of CASPT2 geometries, the structure numbers of corresponding S_0/S_1-MECIs by SF-BHHLYP are shown in parentheses.

Table 1. Comparison of Energies of S_0/S_1-MECIs, Relative to the Ground-State Ethylene at Different Computational Levels[a]

	S_0/S_1-MECIs Energy (eV)				
	SF-BHHLYP/cc-pVDZ[b]	SF-BHHLYP/aug-cc-pVDZ[c]	MS3-CASPT2/cc-pVDZ[b]	MS2-CASPT2/6-31G(d,p)[d]	MR-CISD+Q/aug-cc-pVDZ[e]
twisted-pyramidal	4.74 (4.74)	4.71 (4.73)	4.42 (4.42)	4.81 (4.82)	4.50 (4.54)
ethylidene	4.54 (4.54)	4.47 (4.49)	4.75 (4.75)	4.71 (4.73)	4.56 (4.57)

[a]The energies for the lower and upper states, respectively, are shown before and inside the parentheses. [b]Data taken from this work. [c]Data taken from ref 35. [d]Data taken from ref 14. [e]Data taken from ref 55.

ADDF3 option, which considers the three largest ADDs around each local minimum, was used. ADDF was applied only to minima having bond connectivity that was identical to that of the initial (ethylene or 1,3-butadiene) structure. This does not mean that structures with a different bond connectivity will not be found; these structures are found as seen below, although further *l*-ADDF3 searches starting from them are not performed. In ADDF calculations, Hessian is computed at each local minimum of the seam model function to obtain the reference harmonic potential for ADD detection. In this study, Hessians were computed numerically using gradients, where numerical Hessians take just a portion of the entire computation time as numerous gradient calculations are done in the entire ADDF procedure.

All obtained structures via the initial search, i.e., local minima on eq 1 at the SF-BHHLYP/6-31G level, were reoptimized (the second step of SMF) at the SF-BHHLYP and multistate CASPT2 (MS-CASPT2) levels, by the DG method, using the BP-updating procedure. In both computational levels, the cc-pVDZ basis set was employed. In CASPT2 calculations, an active space including 2 electrons and 2 orbitals (2e,2o) and that of (4e,4o) were adopted in ethylene and 1,3-butadiene calculations, respectively, to include all π and π^* orbitals associated with double bonds. In the CASPT2 calculations, the lowest three states were considered (MS3-CASPT2).

The SMF/ADDF/SF-TDDFT calculations were performed by a local developmental version of the GRRM program,[73] in which a code connecting the GRRM program and the GAMESS program[74,75] was developed in this study. All geometrical displacements were treated by GRRM using SF-TDDFT gradients obtained by GAMESS and CASPT2 gradients by MOLPRO2010.[76]

IV. RESULTS AND DISCUSSIONS

A. Ethylene. In the application to ethylene, two, seven, and three MESXs were found for PES-I/PES-II, PES-II/PES-III, and PES-III/PES-IV, respectively, as listed in Figures 2a–c. In the automated SMF/*l*-ADDF3 search, 14 283 gradients were computed in total. In Figure 2, these structures are sorted in the order of relative energies, and the energies and the values of $\langle S^2 \rangle$ are also shown (values shown in square brackets in the figure). As shown in Figure 2, the values of $\langle S^2 \rangle$ are deviated from the ideal values as mentioned previously. Nevertheless, it is not difficult to identify S_0/S_1-MECIs from the structure list. Structures **3** and **4** correspond to S_0/S_1-MECIs, as the $\langle S^2 \rangle$ values of both PES-II and PES-III are close to zero. This assignment is supported by two S_0/S_1-MECIs (**13** and **14**), obtained by CASPT2 and shown in Figure 2d. These have been previously reported as S_0/S_1-MECIs of ethylidene and twisted-pyramidal types, respectively.[14,35,51,55−57] It follows that the automated search for S_0/S_1-MECIs was successful. The remaining MESXs by SF-BHHLYP can be classified into S_0/T_1-MESXs, S_1/T_1-MESXs, and those involving the singlet/triplet mixed states. Although S_0/T_1-MESXs and S_1/T_1-MESXs are also useful in discussions of intersystem crossing pathways, further evaluation of these structures by CASPT2 was not

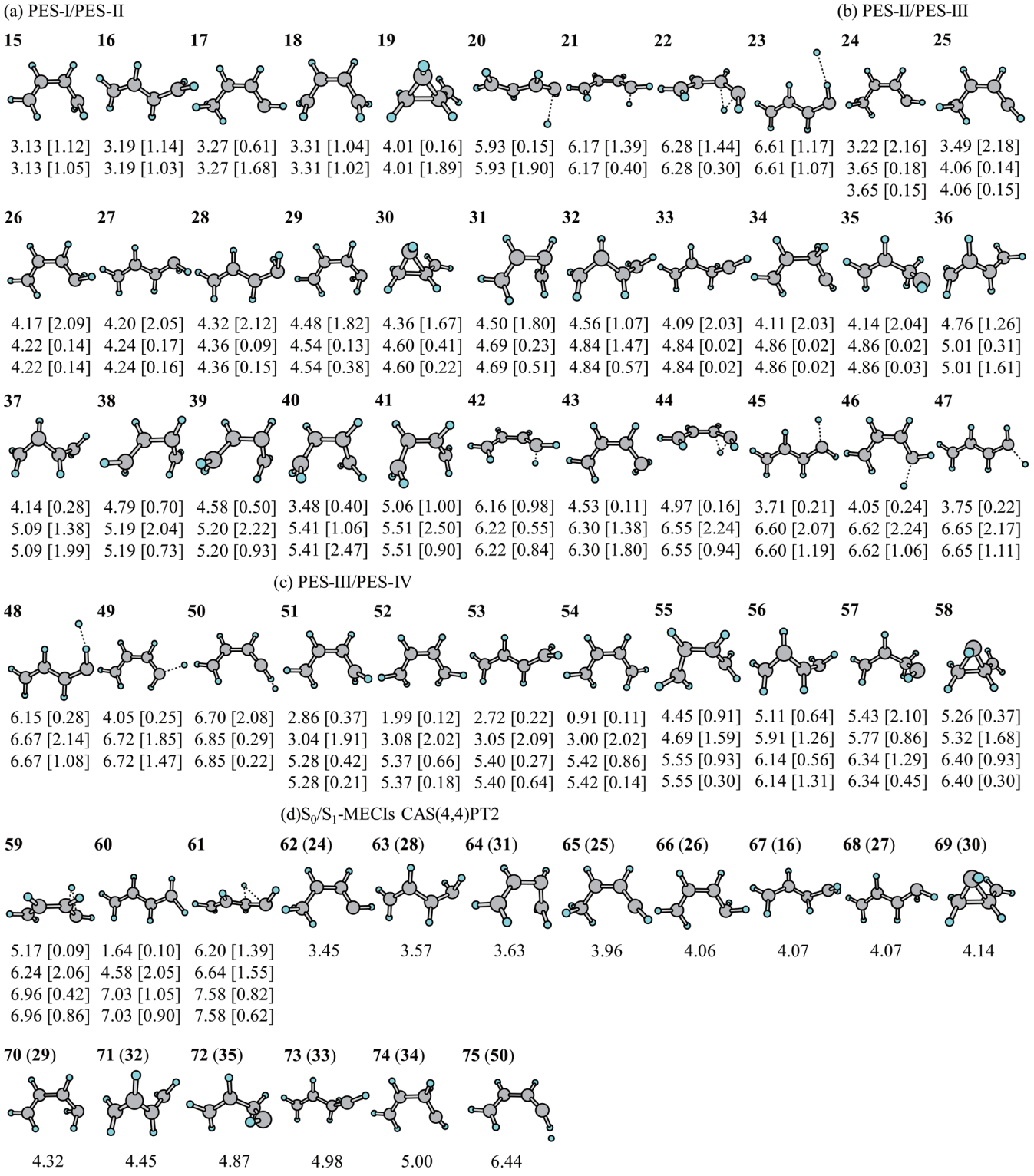

Figure 3. Structures and energies of lowest two to four states at the optimized MESXs (including MECIs) at the SF-BHHLYP/cc-pVDZ level and at the optimized S_0/S_1-MECIs at the MS3-CAS(4e,4o)PT2/cc-pVDZ level for C_4H_6: (a) PES-I/PES-II MESXs at the SF-BHHLYP/cc-pVDZ level, (b) PES-II/PES-III MESXs at the SF-BHHLYP/cc-pVDZ level, (c) PES-III/PES-IV MESXs at the SF-BHHLYP/cc-pVDZ level, and (d) S_0/S_1-MECIs at the CASPT2 level. Energies (in eV) are relative to the ground-state *trans*-1,3-butadiene, and $\langle S^2 \rangle$ values for corresponding states are shown in square brackets. In structure labels of CASPT2 geometries, the numbers of corresponding S_0/S_1-MECIs by SF-BHHLYP are shown in parentheses.

considered in this study, because the focus of the present study is finding S_0/S_1-MECIs.

As mentioned previously, the S_0/S_1-MECI geometries at the BHHLYP/cc-pVDZ level (**3** and **4** in Figure 2) are very similar to those by CASPT2 (**14** and **13**, respectively). The accuracy of the relative energies should be also mentioned. In Table 1, energies relative to the ground-state ethylene molecule at different computation levels are tabulated for S_0/S_1-MECIs of the twisted-pyramidal types (**4** and **13**) and ethylidene types (**3** and **14**). The present SF-TDDFT results reproduce the

dx.doi.org/10.1021/ct400512u | J. Chem. Theory Comput. 2013, 9, 4116−4123

previous ones using the same functional very well.[35] Moreover, deviations from the present and previous CASPT2 and MRCI energies[14,55] are also small, as discussed in ref 35.

B. Butadiene. By the SMF/*l*-ADDF3 search, 9, 27, and 11 MESX structures were found for PES-I/PES-II, PES-II/PES-III, and PES-III/PES-IV, respectively, as shown in Figures 3a−c. Energies relative to the ground-state *trans*-1,3-butadiene and the values of $\langle \mathbf{S}^2 \rangle$ are also shown (values are shown in square brackets in the figure). In Figures 3a−c, the structures are shown in the order of the relative energies. The total number of gradient calculations required in the SMF/*l*-ADDF3 search was 64 323.

We assigned structures **16**, **24**−**35**, and **50** in Figure 3 to be S_0/S_1-MECIs. All of these, except for structures **16** and **29**−**32**, can be classified as S_0/S_1-MECIs, easily based on the $\langle \mathbf{S}^2 \rangle$ values of PES-II and PES-III. Although structures **29**−**31** show relatively large $\langle \mathbf{S}^2 \rangle$ values (∼0.5), these may also correspond to S_0/S_1-MECIs. These assignments can be justified by comparing these geometries to the optimized S_0/S_1-MECI structures at the MS3-CAS(4e,4o)-PT2/cc-pVDZ level shown in Figure 3d, where in structure labels, the structure numbers of corresponding SF-TDDFT geometries are designated. Structures **16** and **32**, which are crosses between two singlet/triplet mixed states, can be compared with S_0/S_1-MECIs **67** and **71** at the CASPT2 level, since these are similar both energetically and geometrically. Therefore, we finally assigned structures **16** and **32** to be S_0/S_1-MECIs.

It should be emphasized that we were able to obtain all S_0/S_1-MECIs in Figure 3d, starting from SF-TDDFT geometries. It follows that the SMF/*l*-ADDF3/SF-TDDFT search is powerful for finding MECI geometries automatically without using any guessing. As discussed, one can classify most of SF-TDDFT structures as S_0/S_1-MECIs and others based on the $\langle \mathbf{S}^2 \rangle$ values. In order not to overlook any S_0/S_1-MECI, further examination by other methods such as CASPT2 is recommended, as has been done in this study. As mentioned above, further evaluation of S_0/T_1-MESXs and S_1/T_1-MESXs by CASPT2 was not considered in this study.

The relative energies shown in Figures 3a−c are in moderate agreement with those obtained by MS-CASPT2, shown in Figure 3d. With regard to S_0/S_1-MECIs, the largest difference of relative energies is 1.06 eV (between that of structure **64** and that of structure **31**). This may be in part because of the choice of the BHHLYP functional and also in part due to the small (4e,4o) active space employed in the MS-CASPT2 calculations. Nevertheless, evaluating the functional dependence as well as obtaining highly accurate energetics via extensive ab initio calculations is outside the scope of this study; the present focus is finding S_0/S_1-MECI geometries.

Some structures in Figures 3a−c correspond to those obtained in previous studies: cisoid **31** (**64**),[15,42−44,46,48,49,52−54,60,61] transoid **32** (**71**),[14,32,42,43,45,52−54,60,62,65] pyramidal **26**−**29** (**66**, **68**, **63**, and **70**),[14,32,50,62] and methylenecyclopropane **30** (**69**),[50,60,64] and twisted **16** (**67**).[14,32,62] Some new S_0/S_1-MECIs were also found. To our knowledge, among structures confirmed at the CASPT2 level, **24** (**62**), **25** (**65**), **33** (**73**), **34** (**74**), **35** (**72**), and **50** (**75**) have not been reported. These can be compared with ethylidene[14,35,47,51,55−58] for C_2H_4 (see **3** and **14** in Figure 2), where **33**−**35** involve a 1−2 hydrogen transfer, **24** and **25** involve a 1−4 hydrogen transfer, and **50** involves a H-atom dissociation. On the other hand, cyclobutene type[63] was not found in the present restricted search using the *l*-ADDF3 and bond-connectivity restrictions. In the reported cyclobutene-type MECI, one H-atom is dissociated.[63] Thus, it can be reached after rearrangements of at least two chemical bonds: C−C bond formation and C−H bond dissociation. Structures involving rearrangements of two or more chemical bonds from the 1,3-butadiene structure are not found in the present search using the bond-connectivity restriction. Although, in principle, one can apply the present method without this restriction, the computational costs will increase dramatically. Moreover, it is not beneficial to locate MECIs highly deviated from the initial FC structure in the study of actual photochemical reactions. Thus, we conclude that the present SMF/*l*-ADDF3/SF-TDDFT search located automatically all reported and some new S_0/S_1-MECIs relevant to photochemistry of 1,3-butadiene.

As shown in Figures 2 and 3, the present method gives not only S_0/S_1-MECIs but also S_1/S_2-MECIs and MESXs, including triplet and/or unphysical mixed states. With regard to butadiene, 14 out of 47 MESX structures correspond to S_0/S_1-MECIs. For ethylene only, two out of 12 MESX structures are S_0/S_1-MECIs. Obviously, calculations of unwanted MESX structures can be avoided if a multireference method is employed, instead of SF-TDDFT. However, the use of SF-TDDFT is still beneficial in large systems. This is because the costs of single-gradient calculations by multireference methods grow much more rapidly, depending on the system size, than that for SF-TDDFT. In very large systems, with multireference methods, even single-point calculations can be highly demanding. Thus, we believe that use of SF-TDDFT would greatly improve the applicability of global searches for S_0/S_1-MECIs to large systems.

V. CONCLUSION

Combined SMF/ADDF and SF-TDDFT methods enabled TDDFT-based automated search for S_0/S_1-MECI geometries. The well-known problem of SF-TDDFT—that the response state is not a spin eigenstate—has prevented the automated search of MECIs. To overcome this problem, we proposed a robust strategy, in which crossing seams between all combinations of low-lying states are explored. For instance, the lowest four states, including S_0, S_1, and T_1, were considered in this study. Thus, the output of the automated search is expected to include all S_0/S_1-MECIs. To evaluate the performance of the present method, it was applied to two unsaturated hydrocarbons: ethylene and 1,3-butadiene. In both cases, the SMF/ADDF searches on the PESs of the SF-TDDFT method automatically gave all reported and some new S_0/S_1-MECI geometries, relevant to the photochemistry of these molecules; this was subsequently confirmed by CASPT2.

We would comment on limitations of the current SF-TDDFT. First, as discussed in section II.C, it can only describe excitations in the two-electron−two-orbital active space. Although the convergence of SF-TDDFT equation fails when one of eigenvalues (excitation energies from the triplet reference) is close to zero, this problem can be removed by using the diagonal shift parameter. Because the current SF-TDDFT is a type of linear-response TDDFT within the adiabatic approximation, the problems applied to the standard TDDFT are also true. However, the problem concerned with description of charge-transfer (CT) states is expected to be less severe, compared to the standard TDDFT, because the present collinear SF-TDDFT calculation employs a relatively high mixing weight of Hartree−Fock exchange, namely, BHHLYP. The CT problem can be further reduced by implementations of

the range-separated functionals and/or noncollinear approximation to the SF-TDDFT in the future.

The most significant merit of SF-TDDFT for the present purpose is that it can describe the S_0/S_1-CI intersection, as well as its branching plane, appropriately. This allowed us to explore S_0/S_1-MECIs efficiently by combining the SMF/ADDF method with the SF-TDDFT method, because the cost of SF-TDDFT is still similar to that of the standard TDDFT. The present SMF/ADDF/SF-TDDFT method would be especially useful in large systems to which multireference methods such as CASSCF and CASPT2 are not readily applicable. Thus, applications to larger systems will be a future subject.

■ ASSOCIATED CONTENT

Supporting Information

Cartesian coordinates for all structures shown in Figures 2 and 3. This material is available free of charge via the Internet at http://pubs.acs.org.

■ AUTHOR INFORMATION

Corresponding Author

*E-mail addresses: smaeda@mail.sci.hokudai.ac.jp (S.M.), morokuma@fukui.kyoto-u.ac.jp (K.M.).

Notes

The authors declare no competing financial interest.

■ ACKNOWLEDGMENTS

Y. H. thanks a support from the Japan Society for the Promotion of Science for Research Fellowships for Young Scientist. This work is partly supported by grants from Japan Society for the Promotion of Science (Grants-in-Aid for Scientific Research ⟨KAKENHI⟩, No. 23685004 at Hokkaido University and No. 24245005 at Kyoto University). Some of the calculations were performed using the computational resources at Institute for Molecular Science (Okazaki, Japan).

■ REFERENCES

(1) Bernardi, F.; Olivucci, M.; Robb, M. A. *Chem. Soc. Rev.* **1996**, *25*, 321−328.
(2) Yarkony, D. R. *Acc. Chem. Res.* **1998**, *31*, 511−518.
(3) Schroder, D.; Shaik, S.; Schwarz, H. *Acc. Chem. Res.* **2000**, *33*, 139−145.
(4) Sobolewski, A. L.; Domcke, W.; Dedonder-Lardeux, C.; Jouvet, C. *Phys. Chem. Chem. Phys.* **2002**, *4*, 1093−1100.
(5) Poli, R.; Harvey, J. N. *Chem. Soc. Rev.* **2003**, *32*, 1−8.
(6) Levine, B. G.; Martinez, T. J. *Annu. Rev. Phys. Chem.* **2007**, *58*, 613−634.
(7) Nanbu, S.; Ishida, T.; Nakamura, H. *Chem. Sci.* **2010**, *1*, 663−674.
(8) Koga, N.; Morokuma, K. *Chem. Phys. Lett.* **1985**, *119*, 371−374.
(9) Manaa, M. R.; Yarkony, D. R. *J. Chem. Phys.* **1993**, *99*, 5251−5256.
(10) Bearpark, M. J.; Robb, M. A.; Schlegel, H. B. *Chem. Phys. Lett.* **1994**, *223*, 269−274.
(11) Anglada, J. M.; Bofill, J. M. *J. Comput. Chem.* **1997**, *18*, 992−1003.
(12) Ciminelli, C.; Granucci, G.; Persico, M. *Chem.—Eur. J.* **2004**, *10*, 2327−2341.
(13) Keal, T. W.; Koslowski, A.; Thiel, W. *Theor. Chem. Acc.* **2007**, *118*, 837−844.
(14) Levine, B. G.; Coe, J. D.; Martinez, T. J. *J. Phys. Chem. B* **2008**, *112*, 405−413.
(15) Sicilia, F.; Blancafort, L.; Bearpark, M. J.; Robb, M. A. *J. Chem. Theory Comput.* **2008**, *4*, 257−266.
(16) Maeda, S.; Ohno, K.; Morokuma, K. *J. Chem. Theory Comput.* **2010**, *6*, 1538−1545.
(17) Maeda, S.; Ohno, K.; Morokuma, K. *Phys. Chem. Chem. Phys.* **2013**, *15*, 3683−3701.
(18) Ohno, K.; Maeda, S. *Chem. Phys. Lett.* **2004**, *384*, 277−282.
(19) Maeda, S.; Ohno, K. *J. Phys. Chem. A* **2005**, *109*, 5742−5753.
(20) Ohno, K.; Maeda, S. *J. Phys. Chem. A* **2006**, *110*, 8933−8941.
(21) Maeda, S.; Morokuma, K. *J. Chem. Phys.* **2010**, *132*, 241102/1−241102/4.
(22) Maeda, S.; Komagawa, S.; Uchiyama, M.; Morokuma, K. *Angew. Chem., Int. Ed.* **2011**, *50*, 644−649.
(23) Maeda, S.; Morokuma, K. *J. Chem. Theory Comput.* **2011**, *7*, 2335−2345.
(24) Maeda, S.; Ohno, K.; Morokuma, K. *J. Phys. Chem. A* **2009**, *113*, 1704−1710.
(25) Maeda, S.; Saito, R.; Morokuma, K. *J. Phys. Chem. Lett.* **2011**, *2*, 852−857.
(26) Maeda, S.; Ohno, K.; Morokuma, K. *Adv. Chem. Phys.* **2012**, *2012*, 268124/1−268124/13.
(27) Mori, T.; Kato, S. *Chem. Phys. Lett.* **2009**, *476*, 97−100.
(28) Gozem, S.; Krylov, A. I.; Olivucci, M. *J. Chem. Theory Comput.* **2013**, *9*, 284−292.
(29) Runge, E.; Gross, E. K. U. *Phys. Rev. Lett.* **1984**, *52*, 997−1000.
(30) Casida, M. E. In *Recent Advances in Density Functional Methods*; Chong, D. P., Ed.; World Scientific: Singapore, 1995; Vol. *1*, pp 155.
(31) Burke, K.; Werschnik, J.; Gross, E. K. U. *J. Chem. Phys.* **2005**, *123*, 062206/1−062206/9.
(32) Levine, B. G.; Ko, C.; Quenneville, J.; Martinez, T. J. *Mol. Phys.* **2006**, *104*, 1039−1051.
(33) Shao, Y. H.; Head-Gordon, M.; Krylov, A. I. *J. Chem. Phys.* **2003**, *118*, 4807−4818.
(34) Wang, F.; Ziegler, T. *J. Chem. Phys.* **2004**, *121*, 12191−12196.
(35) Minezawa, N.; Gordon, M. S. *J. Phys. Chem. A* **2009**, *113*, 12749−12753.
(36) Huix-Rotllant, M.; Natarajan, B.; Ipatov, A.; Wawire, C. M.; Deutsch, T.; Casida, M. E. *Phys. Chem. Chem. Phys.* **2010**, *12*, 12811−12825.
(37) Rinkevicius, Z.; Vahtras, O.; Agren, H. *J. Chem. Phys.* **2010**, *133*, 114104/1−114104/13.
(38) Li, Z.; Liu, W. *J. Chem. Phys.* **2012**, *136*, 024107/1−024107/14.
(39) Bernard, Y. A.; Shao, Y.; Krylov, A. I. *J. Chem. Phys.* **2012**, *136*, 204103/1−204103/17.
(40) Isegawa, M.; Truhlar, D. G. *J. Chem. Phys.* **2013**, *138*, 134111/1−134111/13.
(41) Squillacote, M.; Semple, T. C. *J. Am. Chem. Soc.* **1990**, *112*, 5546−5551.
(42) Olivucci, M.; Ragazos, I. N.; Bernardi, F.; Robb, M. A. *J. Am. Chem. Soc.* **1993**, *115*, 3710−3721.
(43) Olivucci, M.; Bernardi, F.; Ottani, S.; Robb, M. A. *J. Am. Chem. Soc.* **1994**, *116*, 2034−2048.
(44) Celani, P.; Bernardi, F.; Olivucci, M.; Robb, M. A. *J. Chem. Phys.* **1995**, *102*, 5733−5742.
(45) Celani, P.; Garavelli, M.; Ottani, S.; Bernardi, F.; Robb, M. A.; Olivucci, M. *J. Am. Chem. Soc.* **1995**, *117*, 11584−11585.
(46) Bernardi, F.; Olivucci, M.; Robb, M. A. *J. Photochem. Photobiol., A* **1997**, *105*, 365−371.
(47) Freund, L.; Klessinger, M. *Int. J. Quantum Chem.* **1998**, *70*, 1023−1028.
(48) Sakai, S. *Chem. Phys. Lett.* **1998**, *287*, 263−269.
(49) Garavelli, M.; Frabboni, B.; Fato, M.; Celani, P.; Bernardi, F.; Robb, M. A.; Olivucci, M. *J. Am. Chem. Soc.* **1999**, *121*, 1537−1545.
(50) Zilberg, S.; Haas, Y. *J. Phys. Chem. A* **1999**, *103*, 2364−2374.
(51) Ben-Nun, M.; Martinez, T. J. *Chem. Phys.* **2000**, *259*, 237−248.
(52) Izzo, R.; Klessinger, M. *J. Comput. Chem.* **2000**, *21*, 52−62.
(53) Sakai, S. *Chem. Phys. Lett.* **2000**, *319*, 687−694.
(54) Garavelli, M.; Bernardi, F.; Olivucci, M.; Bearpark, M. J.; Klein, S.; Robb, M. A. *J. Phys. Chem. A* **2001**, *105*, 11496−11504.
(55) Barbatti, M.; Paier, J.; Lischka, H. *J. Chem. Phys.* **2004**, *121*, 11614−11624.
(56) Barbatti, M.; Granucci, G.; Persico, M.; Lischka, H. *Chem. Phys. Lett.* **2005**, *401*, 276−281.

(57) Barbatti, M.; Ruckenbauer, M.; Lischka, H. *J. Chem. Phys.* **2005**, *122*, 174307/1−174307/7.
(58) Yamazaki, S.; Kato, S. *J. Chem. Phys.* **2005**, *123*, 114510/1−114510/13.
(59) Chen, H.; Li, S. *J. Org. Chem.* **2006**, *71*, 9013−9022.
(60) Sicilia, F.; Blancafort, L.; Bearpark, M. J.; Robb, M. A. *J. Phys. Chem. A* **2007**, *111*, 2182−2192.
(61) Dick, B.; Haas, Y.; Zilberg, S. *Chem. Phys.* **2008**, *347*, 65−77.
(62) Levine, B. G.; Martinez, T. J. *J. Phys. Chem. A* **2009**, *113*, 12815−12824.
(63) Rossi, A. R.; Wang, Y.; Wiberg, K. B. *J. Phys. Chem. A* **2009**, *113*, 1686−1695.
(64) Snyder, J. W., Jr.; Mazziotti, D. A. *J. Chem. Phys.* **2011**, *135*, 024107/1−024107/8.
(65) West, A. C.; Windus, T. L. *Theor. Chem. Acc.* **2012**, *131*, 1251/1−1251/11.
(66) Fukui, K. *J. Phys. Chem.* **1970**, *74*, 4161−4163.
(67) Maeda, S.; Ohno, K. *J. Phys. Chem. A* **2007**, *111*, 4527−4534.
(68) Yamaguchi, K.; Tsunekawa, T.; Toyoda, Y.; Fueno, T. *Chem. Phys. Lett.* **1988**, *143*, 371−376.
(69) Shoji, M.; Koizumi, K.; Kitagawa, Y.; Kawakami, T.; Yamanaka, S.; Okumura, M.; Yamaguchi, K. *Chem. Phys. Lett.* **2006**, *432*, 343−347.
(70) Xu, X.; Gozem, S.; Olivucci, M.; Truhlar, D. G. *J. Phys. Chem. Lett.* **2013**, *4*, 253−258.
(71) Becke, A. D. *Phys. Rev. A* **1988**, *38*, 3098−3100.
(72) Lee, C. T.; Yang, W. T.; Parr, R. G. *Phys. Rev. B* **1988**, *37*, 785−789.
(73) Maeda, S.; Osada, Y.; Harabuchi, Y.; Taketsugu, T.; Morokuma, K.; Ohno, K. *GRRM, a developmental version*; Hokkaido University: Sapporo, Japan, 2013.
(74) Schmidt, M. W.; Baldridge, K. K.; Boatz, J. A.; Elbert, S. T.; Gordon, M. S.; Jensen, J. H.; Koseki, S.; Matsunaga, N.; Nguyen, K. A.; Su, S. J.; Windus, T. L.; Dupuis, M.; Montgomery, J. A. *J. Comput. Chem.* **1993**, *14*, 1347−1363.
(75) Gordon, M. S.; Schmidt, M. W. In *Theory and Applications of Computational Chemistry: The First Forty Years*; Dykstra, C. E., Frenking, G., Kim, K. S., Scuseria, G. E., Eds.; Elsevier: Amsterdam, The Netherlands, 2005; p 1167.
(76) Werner, H.-J.; Knowles, P. J.; Knizia, G.; Manby, F. R.; Schutz, M.; Celani, P.; Korona, T.; Lindh, R.; Mitrushenkov, A.; Rauhut, G.; Shamasundar, K. R.; Adler, T. B.; Amos, R. D.; Bernhardsson, A.; Berning, A.; Cooper, D. L.; Deegan, M. J. O.; Dobbyn, A. J.; Eckert, F.; Goll, E.; Hampel, C.; Hesselmann, A.; Hetzer, G.; Hrenar, T.; Jansen, G.; Koppl, C.; Liu, Y.; Lloyd, A. W.; Mata, R. A.; May, A. J.; McNicholas, S. J.; Meyer, W.; Mura, M. E.; Nicklass, A.; O'Neill, D. P.; Palmieri, P.; Peng, D.; Pfluger, K.; Pitzer, R.; Reiher, M.; Shiozaki, T.; Stoll, H.; Stone, A. J.; Tarroni, R.; Thorsteinsson, T.; Wang, M. *MOLPRO, version 2012.1, a package of ab initio programs*; see http://www.molpro.net (accessed July 14, 2013).